Structure of α-Olefins on Different Solid Surfaces: A Molecular Dynamics Study

ARTICLE *in* THE JOURNAL OF PHYSICAL CHEMISTRY C · AUGUST 2013

Impact Factor: 4.77 · DOI: 10.1021/jp402934j

3 AUTHORS, INCLUDING:

Hector Dominguez

Universidad Nacional Autónoma de México

53 PUBLICATIONS **631** CITATIONS

SEE PROFILE

Edgar Núñez-Rojas

Universidad Nacional Autónoma de México

6 PUBLICATIONS **13** CITATIONS

SEE PROFILE

THE JOURNAL OF PHYSICAL CHEMISTRY C

Article

pubs.acs.org/JPCC

Structure of α-Olefins on Different Solid Surfaces: A Molecular Dynamics Study

Deneb Peredo-Mancilla, Hector Dominguez,* and Edgar Núñez-Rojas

Material Research Institute, National Autonomous University of Mexico (UNAM), México, D.F. 04510

ABSTRACT: Molecular dynamics simulations of different α-olefin molecules on different solid surfaces, aluminum, graphite, and silicon dioxide (SiO_2) were carried out. Then, studies of how α-olefins were adsorbed on the different surfaces were conducted in terms of density profiles and angular distributions of the molecules chains. It was found that depending on the solid surface the molecules arrayed in different ways. On the aluminum surface the olefin molecules formed a well-defined layer, next to the wall, adsorbed by the double bond with their tails perpendicular to the surface. On the other hand, the α-olefin molecules close to graphite and SiO_2 surfaces were adsorbed with their chains parallel to the interfaces. Structure of the molecules, next to the surfaces, was also investigated by analyzing pair correlation functions and an order parameter finding that the molecules present a strong structure on the aluminum surface. Finally, the molecule−surface description given by the two potentials was compared, and different structures were observed on the aluminum surface. Since the results obtained with the Buckingham interaction were considered as the correct, then we found the appropriate Lennard-Jones parameters to reproduce similar data to those given by the Buckingham potential.

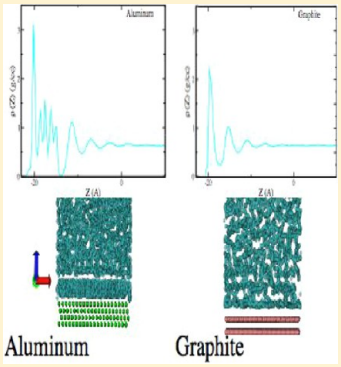

1. INTRODUCTION

The study of organic molecules on solid surfaces is important in order to understand many technological applications; in fact, the interaction between organic molecules and surfaces plays a vital role in areas such as molecular electronics,[1] nanodevices.[2] and molecular recognition.[3] Adsorption and diffusion of oligomers and polymers on metal surfaces are also of interest in areas of friction and lubrication and when organic films are formed on metal electrodes.[4−7] Therefore, different deposition methods have been used to create molecular materials which have been employed to develop solar cells,[8] gas sensors,[9] heterojunctions,[10] and ultrafast optical switches.[11]

Interaction of olefin molecules with several substrates has been studied to investigate adsorption. For instance, in the petrochemical industry,[12] adsorption of olefins on activated carbon surfaces has been studied in order to separate mixtures whereas 1-butene adsorption on uranium oxide has been investigated to study olefin oxidation.[13] In particular, 1-hexene on platinum (111) has been of relevant importance in the production of high-octane fuel.[14] In fact, this molecule has also been studied on gold surfaces due to the usefulness in lubrication, catalysis, and electric contacts.[15] On the other hand, the interaction between alkenes and zeolites has been investigated to understand catalysis and separation processes.[16−18]

In general, adsorption of olefins on silica−alumina catalysts has been studied in order to elucidate cracking catalytic processes.[19] Also, the oligomerization of olefins over amorphous silica−alumina has been investigated with feed materials containing 1−4 oxygenates to determine the effect of the oxygenates on catalyst performance and transportation fuel quality.[20]

As it was mentioned, the interaction molecule−solid is very important since the binding and ordering of molecules on surfaces are generally controlled by a balance between molecule−substrate and intermolecular interactions. Besides, it is considered that solid substrates provide bonds and specific adsorption sites to the molecules.[21−24] In fact, when adsorbing large organic molecules on solid substrates, the complexity of the molecule−surface interaction often increases. For example, several studies have indicated a restructuring of the substrate underneath the molecular adsorbate layer.[25,26]

Because of the chemical simplicity of olefins, molecular simulations could provide a useful complement in the study and description of these systems.[27] However, in order to model interfaces between those molecules and solids, it is necessary to have reliable force fields. Those force fields, for instance, can be obtained by appropriate parametrization of measurements made from first principles calculations such as density functional theory (DFT).[28]

Therefore, few united-atom force fields have appeared in the literature which can accurately describe coexistence curves for normal alkanes[29−31] and branched alkanes[32] and also to study densities, boiling points, heat capacities, and compressibilities.[33] Moreover, force fields have been developed not only to investigate phase equilibrium of α-olefins[34] but also to model properties of mixtures of alkanes and olefins.[27]

In the present work it is described the behavior of α-olefins interacting with different solid surfaces. In particular, we study 1-butene, 1-hexene, 1-octene, and 1-decene on solid surfaces such as aluminum, silicon dioxide, and graphite to investigate

Received: March 25, 2013
Revised: July 16, 2013
Published: July 20, 2013

dx.doi.org/10.1021/jp402934j | J. Phys. Chem. C 2013, 117, 16397−16405

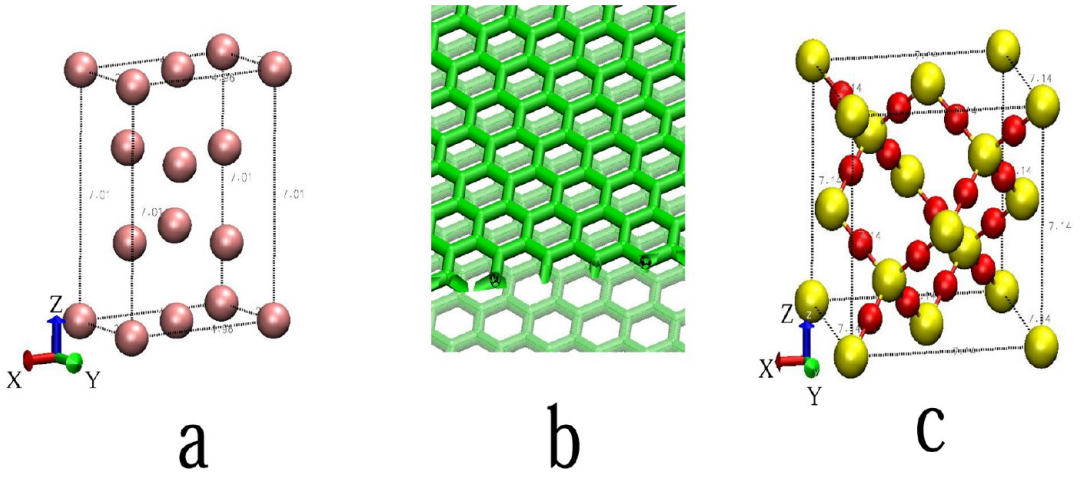

Figure 1. Structures of solid surfaces: (a) unit cell of aluminum surface with (111) orientation, (b) solid surface of hexagonal graphite, and (c) unit cell of silicon dioxide with (001) orientation. Oxygen atoms are red balls, and silicon atoms are yellow balls.

adsorption of the molecules and how they arrange on the different surfaces. Molecular behavior is studied in terms of density profiles, orientation of the hydrocarbon chains, and an order parameter.

2. COMPUTATIONAL METHOD AND MODEL

For the present study molecular dynamics simulations of α-olefin molecules on three different surfaces were carried out.

In Figure 1, we show the unit cell of an aluminum surface with orientation (111) (Figure 1a), carbon atoms on a graphite surface (Figure 1b), and the unit cell of the silicon dioxide surface with orientation (001) (Figure 1c). In all cases the atoms in the solid surfaces were rigid to keep their solid structures.

The aluminum, graphite, and silicon surfaces were constructed with 4, 2, and 5 layers, respectively. It is worthy to mention that for the graphite surface simulations with four and six layers were also tested, and the results did not change significantly.

For the α-olefin systems four different molecules were used—1-butene, 1-hexene, 1-octene, and 1-decene—and they were modeled using a united atom force field.[27] The initial configuration was prepared using 512 α-olefins with the double bond initially pointed to the opposite direction of the solid surface and placed in 8 ordered layers close to the surface.

Two additional tests were performed for each solid surface for the 1-octene molecule by changing the initial configuration: in one case the α-olefins were placed parallel to the solid surface, and in the other case the molecules were arranged vertically. The final configuration in each case had the same behavior, indicating that the initial configuration did not affect the general results.

The usual periodic boundary conditions were imposed in the simulations in a box of dimensions X, Y (see Table 1) whereas the Z dimension of the box was set to 150 Å. This length was long enough to prevent the formation of a second α-olefins/solid interface due to the periodicity of the system. Instead, a liquid/vapor interface was present at one end of the box ($Z > 0$), whereas at the other end of the box ($Z < 0$) beyond the solid surface there was an empty space. In Table 1, the dimensions of the solid walls and the number of molecules used to build them are shown.

Table 1. Spatial Dimensions and Number of Molecules Used To Build the Solid Surfaces

surface	L_x (Å)	L_y (Å)	L_z (Å)	no. of particles
aluminum	52.077	50.111	7.014	1360
graphite	40.523	38.995	3.349	1232
silicon dioxide	43.702	43.702	13.378	576

As it was indicated above, the united atom force field for α-olefins used in the present simulations was developed previously (by Nath et al.[27]). They tested their model with orthobaric densities and saturation pressures given good agreement with experimental results. Therefore, in this work we did not conduct any more tests, and we used the simulation parameters reported by those authors. We only mention the potentials used in that force field.

The inter- and intramolecular potentials for the α-olefins include bond, angular, and torsional potentials described by the equation

$$E = E_{\text{bond}} + E_{\text{ang}} + E_{\text{tor}} + E_{\text{LJ}} + E_{\text{w}} \tag{1}$$

The bond lengths are modeled by a harmonic potential

$$E_{\text{bond}} = \frac{K_{\text{b}}}{2}(r - r_0)^2 \tag{2}$$

where r_0 is the equilibrium distance between two bonded atoms and K_{b} is the bond constant. The angles in the chain are also constrained by the harmonic potential

$$E_{\text{ang}} = \frac{K_\theta}{2}(\theta - \theta_0)^2 \tag{3}$$

where θ_0 is the equilibrium angle and K_θ is the force constant. The torsional angles are modeled by the OPLS potential

$$E_{\text{tor}} = A_0 + A_1(1 + \cos\theta + A_2(1 - \cos(2\theta)) + A_3(1 + \cos(3\theta)) \tag{4}$$

where the A_n are the energy constants. The potential parameters are given in Table 2.

The intermolecular (E_{LJ}) potential for the α-olefins is modeled using the Lennard-Jones potential

dx.doi.org/10.1021/jp402934j | J. Phys. Chem. C 2013, 117, 16397−16405

Table 2. Intramolecular α-Olefin Potential Parameters

group	K_{ang} (kcal/mol rad^2), θ_0 (rad)	torsion (kcal/mol) A_0, A_1, A_2, A_3	K_{bond} (kcal/mol Å^2), r_0 (Å^2)
CH_n–CH_n–CH_n	124.20, 114.0		
CH_n–CH_1=CH_2	124.20, 124.0		
CH_n–CH_n–CH_n–CH_n		0.000, 0.705, −0.135, 1.572	
CH_nCH_2–CH_1=CH_2		0.095, 0.171, −0.218, 0.560	
CH_n–CH_n			191.76, 1.54
CH_1=CH_2			191.76, 1.34

$$U_{lj}(r_{ij}) = 4\varepsilon\left(\left(\frac{\sigma}{r_{ij}}\right)^{12} - \left(\frac{\sigma}{r_{ij}}\right)^{6}\right) \quad (5)$$

where ε is the lowest value of the potential energy, σ is the distance where the pair potential is zero, and r_{ij} is the distance between two particles.

The Lorentz–Berthelot combining rules are employed for the interaction between unlike pairs

$$\sigma_{ij} = \frac{1}{2}(\sigma_{ii} + \sigma_{ij}) \quad (6)$$

and

$$\varepsilon_{ij} = \sqrt{\varepsilon_{ii}\varepsilon_{jj}} \quad (7)$$

The Lennard-Jones parameters used in the simulations are shown in Table 3.

Table 3. LJ Intermolecular Potential Parameters

site	σ (Å)	ε (kcal/mol)
	α-olefin	
CH_3 (sp^3)	3.91	0.207
CH_2 (sp^3)	3.93	0.091
CH_1 (sp^2)	3.77	0.091
CH_2 (sp^2)	3.72	0.184
	solid surface	
Al (aluminum)	2.620	9.04370
C (graphite)	3.400	0.056
Si (SiO_2)	4.290	0.025
O (SiO_2)	3.300	0.019

For the interaction between α-olefins and solid surfaces (E_w) two different potentials were used. For graphite and silicon dioxide the Lennard-Jones potential (eq 5) was used, whereas for the α-olefin–aluminum interaction LJ and Buckingham potentials were tested. The form of the Buckingham potential has the expression

$$U_{lj}(r_{ij}) = A\exp\left(\frac{-r_{ij}}{\rho}\right) - \left(\frac{C}{r_{ij}^{6}}\right) \quad (8)$$

where A is a constant related to the number of electrons, ρ is also a constant that depends of the electronic density, and C represents the van der Waals interaction; their values are summarized in Table 4 which were taken from ref 28.

Table 4. Buckingham Intermolecular Potential Parameters for the Interaction α-Olefins–Aluminum

pair	A (kcal/mol)	ρ (Å)	C (Å^6 kcal/mol)
Al–CH_n (sp^2)	25686.0	0.392	8018.2
Al–CH_n (sp^3)	8725.5	0.473	5653.1

As stated before, the atoms in the surfaces remained rigid and there were not interactions between them. They only interacted with the α-olefin molecules.

Since graphite walls are composed mainly by carbon atoms, we use the Lennard-Jones parameters for carbon which were taken from refs 35 and 36. In this case the graphite surface thickness was 3.34 Å; however, simulations with 10 and 16 Å thickness were also conducted, and any significant changes were observed in the results. For the silicon dioxide surface the Lennard-Jones parameter were taken from ref 37, and the thickness of the slab was 13 Å. For the aluminum–α-olefin molecule interaction the parameters for the Buckingham potential were taken from Kong et al.;[28] however, for the united atom model, we took only the values for the Al–CH_n, i.e., the interactions with the hydrogens were not included. This approximation was considered appropriate since in the united atom model the CH_n groups are joint in one single site, in this model in the carbon. For the Lennard-Jones potential, the parameters were taken from ref 38. In this case, for aluminum, the surface thickness was 7 Å (thicker than the surface used by Kong[28]).

All simulations were carried out in the NVT ensemble with a time step of 0.002 ps using the DL-POLY package.[39] Bond lengths were constrained using SHAKE algorithm with a tolerance of 10^{-4}, and the temperature was controlled using the Nose–Hoover thermostat[40] with a relaxation time of 0.2 ps at T = 298 K and using a cutoff of 16 Å . In total, all simulations were run for 3 ns, where the last 1 ns was used to data analysis.

3. RESULTS

In this section the calculations performed on the α-olefins on the three different surfaces are shown. Also, studies on the behavior of the α-olefins and the interaction at the liquid/solid interfaces are discussed.

3.1. Density Profiles. Previous investigations of 1-hexene on aluminum suggested that the Buckingham potential is an appropriate potential to study the solid–molecule interaction.[28] Therefore, we start our simulations using the Buckingham potential. Then the first analysis was conducted to calculate the atomic Z-dependent density profiles per CH_n normal to the liquid/solid interface in order to see where the α-olefins molecules arranged in the system.

Figure 2 shows the density profiles calculated along the Z-direction for the four different α-olefin molecules interacting with the aluminum surface (111). From that figure it is observed that, in all the cases, a layer of α-olefin molecules on the surface is formed. It is even possible to observe a peak close to the surface that is about twice as high as the others. By observing the high of the first peak, it suggests the presence of two CH_n sites per molecule in the proximity of the surface while the other peaks correspond to the remaining sites (CH_n) of the molecules distributing along the Z-direction. These profiles indicate that the molecules in the adsorbed layer are placed vertically attached to the surface by two molecular sites; in fact, they are attached by the double bonded atoms as previous works observed.[41]

dx.doi.org/10.1021/jp402934j | J. Phys. Chem. C 2013, 117, 16397–16405

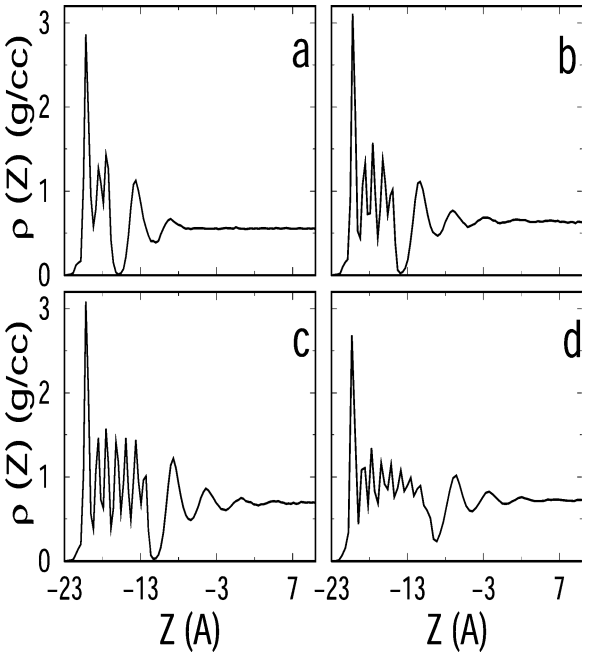

Figure 2. *Z*-density profile for the system α-olefin/aluminum: (a) 1-butene, (b) 1-hexene, (c) 1-octene, and (d) 1-decene.

A few years ago Kong et al.[28] studied α-olefin molecules on aluminum surfaces, and even when it is not clear that they found the same structure it is possible to observe, from their results (snapshots), that there is an adsorbed layer of molecules on the surface. However, in a second paper by the same authors[41] they observed a perpendicular structure of 1-hexene molecules on aluminum surfaces as we report in this work.

Following the formation of the adsorbed layer, it is observed a gap where the density goes to zero, suggesting that there is a space above the adsorbed layer where no molecules are present. Moreover, from those profiles it is also possible to observe the formation of a second (even a third) layer as indicated by the following peaks. Far from the solid surface, the α-olefin molecules did not interact with the solid surface, and we observed a bulk fluid.

Figure 3a shows a snapshot of the final configuration of 1-octene on aluminum; there, it is easy to observe the vertical arrangement of the molecules over the solid surface. Similar configurations were depicted for all α-olefin−aluminum systems.

The following analysis was conducted for the same fluids with the other surfaces. However, for these studies the molecule−solid interactions were calculated with the LJ potential. In Figure 4, the density profiles of the α-olefins on the graphite surface are shown. The molecules are also arranged in layers close to the surface; however, in this case the profiles suggest that the molecules are adsorbed parallel to the surface. Interesting from those profiles is that the number of layers for 1-butene, 1-hexene, and 1-octane are nearly the same, whereas for decene we clearly observe the formation of more layers. Far from the surface the same bulk fluid is depicted as in Figure 2.

A typical arrangement of the molecules is shown in the snapshot of the final configuration of 1-octene on the graphite surface (Figure 3b) where an adsorbed layer next to the solid surface is observed. Moreover, from that picture it is depicted that molecules arrange parallel to the graphite surface.

Figure 5 shows the density profiles of the α-olefins along the *Z*-direction in the proximity of the silicon dioxide surface. There, it is not observed any strong structure of the molecules on the surface; i.e., the peaks that would indicate the formation of adsorbed layers are almost imperceptible in comparison to those observed on the aluminum and the graphite surfaces. Figure 3c shows a snapshot of the last configuration of 1-octene/silicon dioxide in the neighborhood of the solid surface where it is not possible to observe any strong layer. The same configuration is also observed for 1-butene, 1-hexene, and 1-

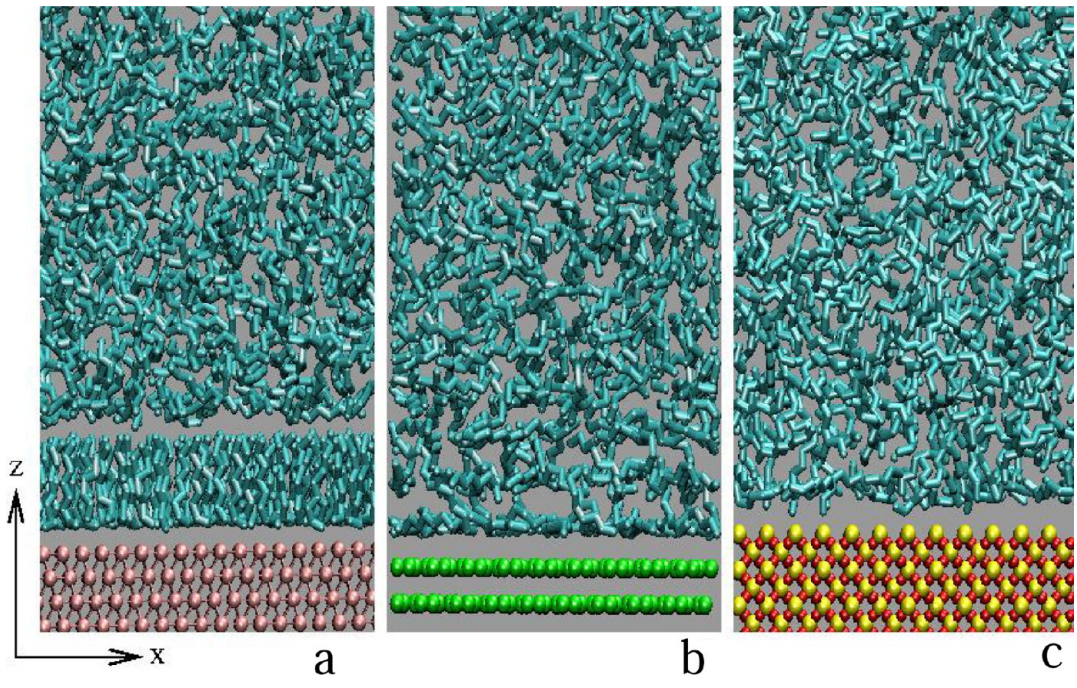

Figure 3. Snapshot of the final configuration of the 1-octene molecules on the solid surfaces: (a) aluminum, (b) graphite, and (c) silicon dioxide.

dx.doi.org/10.1021/jp402934j | J. Phys. Chem. C 2013, 117, 16397−16405

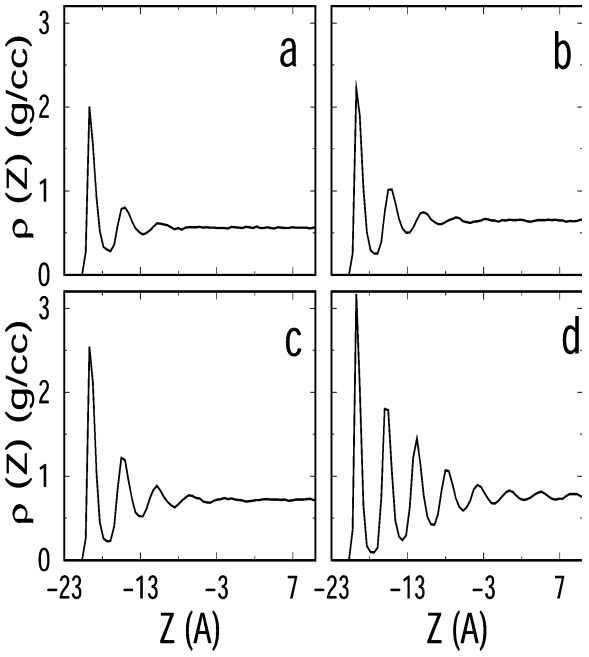

Figure 4. *Z*-density profile for the system α-olefin/graphite: (a) 1-butene, (b) 1-hexene, (c) 1-octene, and (d) 1-decene.

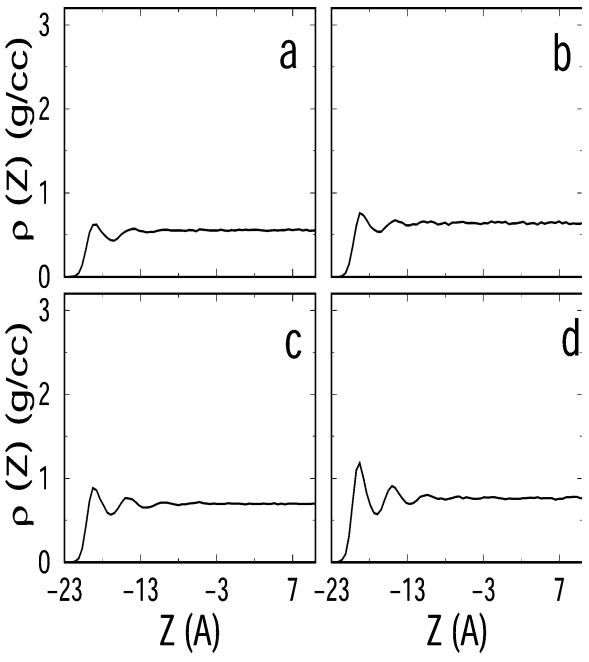

Figure 5. *Z*-density profile for the system α-olefin/silicon dioxide: (a) 1-butene, (b) 1-hexene, (c) 1-octene, and (d) 1-decene.

decene. As the other systems, a bulk fluid is also observed far from the solid surfaces.

3.2. Structural Analysis of Molecules Adsorbed on the Solid Surfaces. It is also possible to analyze how the alkene molecules array within each first adsorbed layer by calculating pair correlation functions $g(r)$ over the center of mass of the molecules (Figure 6).

As a general feature it is observed that the molecules over the aluminum surface present strong peaks, suggesting a solidlike structure. In fact, for the 1-butene the molecules seem to form a

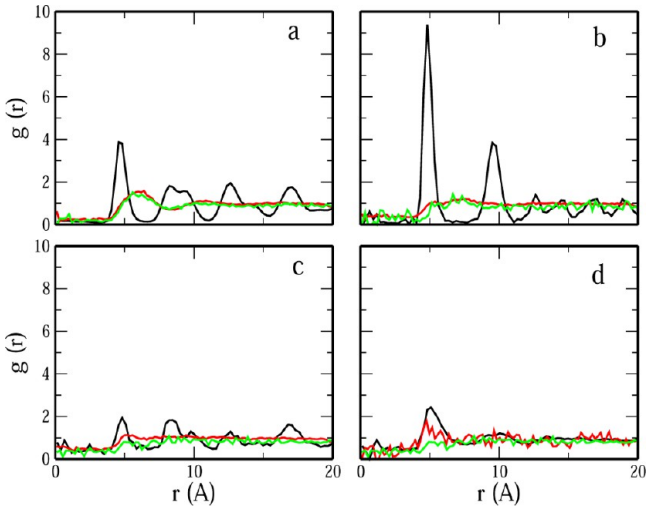

Figure 6. $g(r)$ for center of mass of the different α-olefin molecules of the adsorbed layer on the solid surfaces: (a) 1-butene, (b) 1-hexene, (c) 1-octene, and (d) 1-decene. The black solid line is for the aluminum surface, the red line for the graphite surface, and the green line for the SiO_2 surface.

2-D hexagonal crystal array (see Figure 6a). For molecules far from the surface it was not observed any particular structure.

In the case of α-olefins on graphite and silicon dioxide the $g(r)$ oscillates around 1, indicating that in this surfaces the molecules do not present much structure on the surface. In fact, for the long chains (1-hexene, 1-octane, and 1-decene) the $g(r)$ shows that the centers of mass of the molecules are not close to each other since the pair correlations rapidly decay to unity suggesting a 2D-fluid of very low density.

How the α-olefins accommodate on the different surfaces is also analyzed by measuring the ratio between the nearest-neighbors distance in the substrates with the nearest-neighbors distance of the molecules in the first adsorbed layer (from the center of mass of the molecules given by the first peak in the $g(r)$ of Figure 6). Somehow this ratio gives us information about how commensurate the systems are. Here we only mention the results for the 1-butane molecule since it was the molecule which present the stronger structure on aluminum. The ratio between the nearest-neighbor distance of the aluminum particles (2.86 Å) with the α-olefins (4.8 Å) is 1.68, which is similar to the value reported by Kong et al. (1.7).[28] In the case of the graphite, the ratio of the nearest-neighbor distance between carbons in the surface (1.42 Å) and α-olefins (6.2 Å) is 4.37, whereas for the SiO_2 surface the nearest-neighbor distance between two atoms in the solid surface and α-olefins is 2.18. These last values are higher than that for the aluminum; however, the molecules on these surfaces accommodated parallel on the graphite surface and without any defined structure on the SiO_2 wall.

In the case of the α-olefins on the graphite surface we can observe that carbon chains on graphite accommodate between the carbons of the surface as also observed by previous authors in simulations of other molecules with carbon chains on graphite surfaces.[42,43]

Some authors have reported chain structure dependence of molecules with hydrocarbon tails with the temperature; however, those studies were conducted at temperatures close to the melting point. In our simulations we are far from the melting temperature of the simulated α-olefins.[42,44−46] Never-

dx.doi.org/10.1021/jp402934j | J. Phys. Chem. C 2013, 117, 16397−16405

theless, we did some simulations at different temperates (few degrees above of our simulation temperature), and we did not observe any significant changes in the molecule structure as we expected since the temperature was higher than the melting temperature.

3.3. Orientation and Total Length of Hydrocarbon Chains. By studying the orientation and length of the molecules, it is also possible to obtain more insights of how molecules are arrayed at the different surfaces. The length of the hydrocarbon molecules at the adsorbed layer is calculated, and it is measured by the distance from the last to the first carbon atom; the average total length is calculated using the equation

$$\langle \mathbf{R} \rangle = \frac{1}{P}\frac{1}{N}\sum_{i=1}^{N} \Delta \mathbf{r}_i \tag{9}$$

N is the total number of α-olefins molecules, P is the number of configurations of the last nanosecond of simulation, and

$$\Delta \mathbf{r}_i = \sqrt{(\Delta X)_i^2 + (\Delta Y)_i^2 + (\Delta Z)_i^2} \tag{10}$$

where ΔX is the distance from the last to the first carbon atoms in the hydrocarbon chain in the X coordinate. Similar definitions are given for ΔY and ΔZ.

From these calculations it is observed that length of the molecules is shorter on the aluminum surface whereas molecules on graphite and silicon dioxide present longer lengths (see Table 5). It is also observed that for 1-butene and 1-decene the chain lengths in all three surfaces are similar despite of the different array that the molecules present on the surface.

Table 5. Average Total Length of 1-Alkenes Chain (Å) in the Three Studied Surfaces

molecule	aluminum	graphite	SiO_2
1-butene	3.2250	3.4228	3.4325
1-hexene	4.5534	5.7042	5.6056
1-octene	5.9443	7.9024	7.6529
1-decene	9.0869	9.6250	9.5797

The orientation of the hydrocarbon chains in the adsorbed layers with respect to the vector normal to the interface is also calculated by measuring the angle θ using the equation

$$\cos\theta_i = \left(\frac{\Delta z_i}{\Delta \mathbf{r}_i}\right) \tag{11}$$

In Figure 7, the angular distribution of the four different α-olefin chains in the first adsorbed layer are shown. Here, it can be observed a tendency of the chains on aluminum to be parallel to the vector normal to the solid surface. These results indicate that molecules are mostly perpendicular to the solid surface.

In the case of the α-olefins interacting with graphite, the distributions show a higher probability for the molecules to be parallel to the solid surface. Experiments have found by scanning tunneling microscope (STM) and atomic force microscope (AFM) methods that long organic linear molecules are adsorbed parallel to a graphite surface so that the carbon atoms of the α-olefins chains arranged with each carbon atom in a graphite hexagon.[42,44−46]

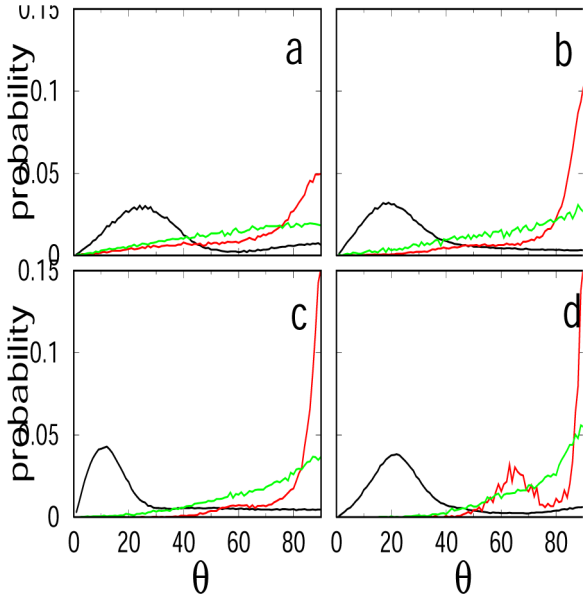

Figure 7. Angular distribution of the molecules on the adsorbed layer of α-olefins chains with respect to the vector normal to the interface: (a) 1-butene, (b) 1-hexene, (c) 1-octene, and (d) 1-decene. The black line is for the aluminum surface, the red line for the graphite surface, and the green line is for the SiO_2 surface.

In Figure 8, a snapshot of the molecules in the adsorbed layer of 1-decene on graphite is shown. Here, it can be observed that the molecules are adsorbed on the hexagonal basal plane.

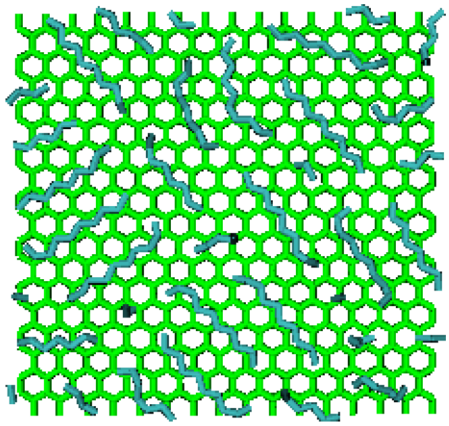

Figure 8. Snapshot of the adsorbed layer of 1-decene on graphite. Since the configuration was cut taking into account the first peak of the density profile, some molecules look incomplete.

Finally, for the interaction with silicon dioxide the angular distributions do not show any particular preference of arrangement for the molecules.

3.4. Order Parameter. In order to obtain more information about the structure of the α-olefin chains in the vicinity of the surface, they are also characterized in terms of an order parameter

$$S_{ij} = \frac{1}{2}\langle 3\cos\theta_i \cos\theta_j - \delta_{ij}\rangle \tag{12}$$

where $i, j = X, Y, Z$ and θ is the angle between the ith molecular axis and the normal to the interface.[47] In this work it is calculated the S_{zz} order parameter since it gives us more

dx.doi.org/10.1021/jp402934j | J. Phys. Chem. C 2013, 117, 16397−16405

information about complete order parallel to the interface (S_{zz} = −0.5) or complete order in the direction normal to interface (S_{zz} = 1.0).

In Figure 9, the S_{zz} values are shown for each set of the α-olefin molecules on the different surfaces. Since the 1-butene

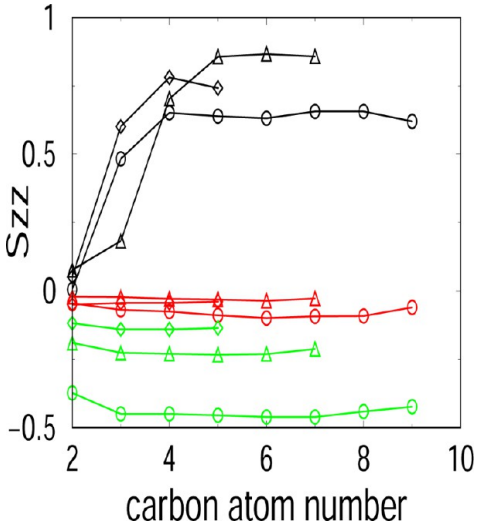

Figure 9. S_{zz} order parameter as a function of carbon position in the hydrocarbon chain of the alkenes on the closest layer to the aluminum surface. Diamonds correspond to 1-hexene, triangles correspond to 1-octene, and circles to 1-decene. The color code is black for the interaction with the aluminum surface, green for the interaction with graphite, and red for the interaction of α-olefins with silicon dioxide.

molecule is too short to obtain relevant information from the S_{zz} parameter, it is not included in the figure. As is observed in Figure 9, the molecules, in the adsorbed layer, on the aluminum surface prefer a vertical orientation. However, the first two atoms (double bond in C_1 and C_2) have values S_{zz} around zero since these two atoms arranged parallel to the surface as indicated in the density profiles.

In the same Figure 9 the result for the α-olefin molecules on the graphite surface (green lines) is also shown. Here, it is observed that the order parameter indicates a preference of the molecules to be parallel to the surface ($S_{zz} \approx -0.5$) for 1-decene atoms. These results are in agreement with the angle distribution and the density profiles data.

The order parameter S_{zz} is also obtained for the first layer at the silicon dioxide surface, and it is also shown in Figure 9 (red lines). In this case the S_{zz} data are very close to the value of zero, suggesting an isotropic orientation of all the molecules in the vicinity of the solid surface.

3.5. Effects on the α-Olefins−Surface Potential. As it was mentioned above, a previous work[28] suggested that the Buckingham potential gives a better description of the interaction between the α-olefins and the aluminum surface. However, in the present work, we also test a LJ potential for the molecule−solid interaction. The LJ parameters for aluminum are given in Table 3, and for the aluminum−α-olefin cross-interaction the Lorentz−Berthelot rules were used.

Figure 10 shows the density profiles of 1-hexene on the aluminum surface using the Buckingham (black line) and the Lennard-Jones potentials (purple line). From that figure it is very clear that the results are different between each other. In fact, the Lennard-Jones potential gives a density profile very similar to that one observed for α-olefins interacting with

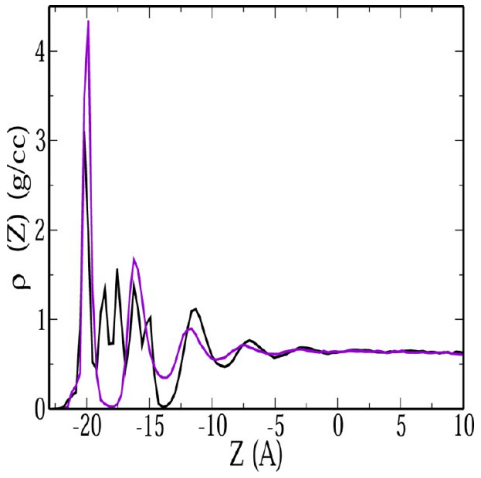

Figure 10. Z-density profile for the system 1-hexene/aluminum surface. The black line was obtained using the Buckingham potential and the purple line using the Lennard-Jones potential with Lorentz−Berthelot combining rules.

graphite (Figure 4) which indicated that the olefin molecules arrayed parallel to the solid surface.

The angular distribution is also obtained for the 1-hexene/aluminum system for both potentials, and it is shown in Figure 11. It is observed that the behavior is opposite for the LJ

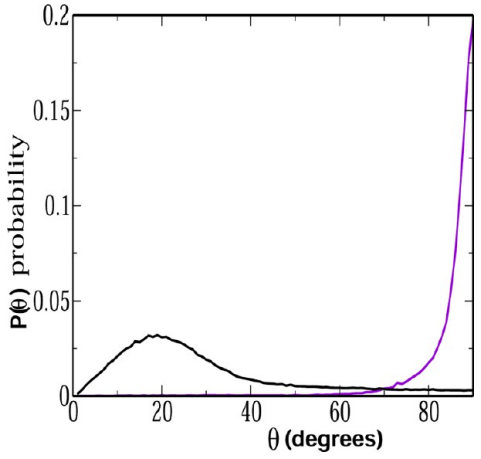

Figure 11. Angular distribution of the molecules on the adsorbed layer for 1-hexene on the aluminum surface. The black line was obtained using the Buckingham potential and the purple line using the Lennard-Jones potential with Lorentz−Berthelot combining rules.

potential. In the case of the Buckingham potential the angular distribution shows the higher probability around 20° while using Lennard-Jones potential the maximum value is around 90°.

It was calculated a new set of LJ parameters to describe the α-olefins−surface interaction by a fitting procedure to match the LJ potential to the Buckingham potential. For the interaction Al−C (sp^2) we found that the new parameters are σ = 3.305 Å and ε = 1.090 kcal/mol while for the interaction Al−C (sp^3) the new parameters are σ = 5.020 and ε = 0.010 kcal/mol.

The density profile obtained with the new Lennard-Jones parameters and the angular distribution are shown in Figures 12 and 13, respectively. Then it is observed that the new results are very alike as the Buckingham potential results.

dx.doi.org/10.1021/jp402934j | J. Phys. Chem. C 2013, 117, 16397−16405

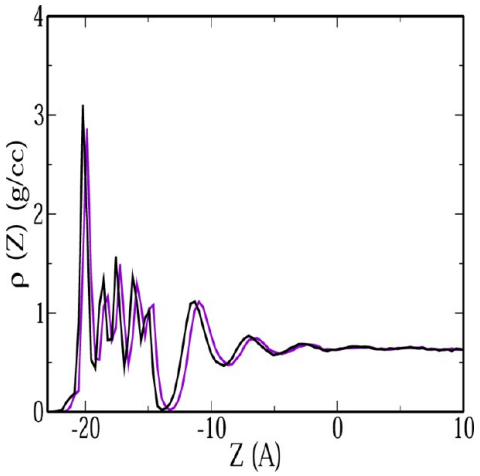

Figure 12. Z-density profile for the 1-hexene/aluminum system. The black line was obtained using the Buckingham potential and the purple line using the Lennard-Jones potential with the new set of parameters for the unlike pairs.

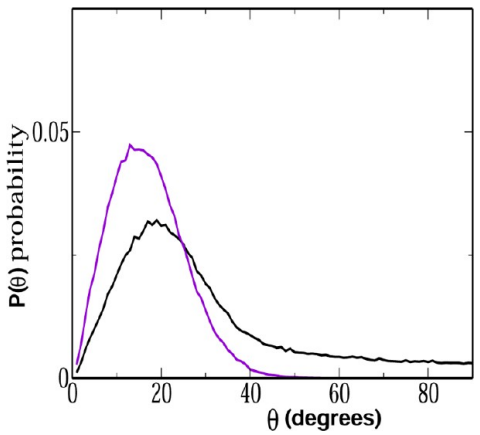

Figure 13. Angular distribution of molecules on the adsorbed layer for 1-hexene on the aluminum surface. The black line was obtained using the Buckingham potential and the purple line using the Lennard-Jones potential with the new set of parameters for the unlike pairs.

3.6. Conclusions. Investigations about the structure of different α-olefins molecules on aluminum, graphite, and SiO_2 surfaces were conducted. It was found that the solid surface had an influence in how α-olefin molecules were adsorbed on the surface. In graphite and SiO_2 surfaces the chains are adsorbed parallel to the solid surfaces. However, in aluminum slabs, the chain molecules are adsorbed perpendicular to the surface. Moreover, the molecules are attached to the solid surface by the double $CH{=}CH_2$ bond, whereas the rest of the CH_n atoms formed a perpendicular chain respect to the surface. This behavior can be understood by the difference in the nature of the carbon atoms in the molecule. Because of the geometry of the double bounded atoms (sp^2), they have more affinity to the aluminum walls than the atoms in the saturated tail (sp^3). The same trends are observed for all the α-olefins investigated; nevertheless, for the 1-hexene the structure of the adsorbed molecules on the surface is even stronger since molecules arrayed in a well-defined 2-D crystal.

From the present results we note that the structure of the α-olefins on aluminum present similar behavior to that describe by Kong et al.[28] Since they used an all atom force field model and we worked with an united atom model, we can say that at this level of information the Al−H potential is not the relevant interaction to describe the structure of the molecules on the surfaces.

From the present results it was found that not only the structure of the surface played and important role to study how the molecules deposited on solid surfaces but also the molecule−solid surface interactions. For instance, for the aluminum surface two molecule−solid interactions were tested, Lennard-Jones and Buckingham, and the results suggested that adsorption was different in the surfaces. Opposite to the Buckingham potential the LJ potential produced parallel adsorption of the molecules. However, by adjusting the Lennard-Jones parameters to have the same form of the Buckingham potential, it is possible to obtain similar results with both interactions; i.e., the molecules next to the surfaces formed a perpendicular structure. It is important to notice that the new Lennard-Jones parameters were only for the molecule−solid interactions; i.e., the Lorentz−Berthelot mixing rules were not used. Therefore, these last results indicated that the Lorentz−Berthelot rules should be used carefully since incorrect values might conduct to a different molecular structure behavior.

We did not find reported data for the α-olefin−graphite and the α-olefin−SiO_2 systems; therefore, the results from these systems should be taken with caution since the cross LJ parameters might not be the better values as in the case of the aluminum. However, if it were the case, we only have to find the new parameters (the cross parameters only) for the solid wall−α-olefin interaction. Nevertheless, we consider that the results of the present work can be trusted since carbon-tails/graphite studies have been studied previously by other authors, and they found, for instance, that tails tend to array parallel on the surface as we observed in our simulations.[42,43]

AUTHOR INFORMATION

Corresponding Author

*E-mail hectordc@unam.mx; Ph 52 (55) 56224604; Fax 52 (55) 56224602 (H.D.).

Notes

The authors declare no competing financial interest.

ACKNOWLEDGMENTS

We acknowledge support from grants DGAPA-UNAM-Mexico, IN102812, and Conacyt-Mexico, 154899. We also thank DGTIC-UNAM for KamBalam supercomputer facilities. D.P.-M. acknowledges the scholarship given by PAPIIT-UNAM trough project IN102812. We also thank the referees for their valuable comments to improve the manuscript.

REFERENCES

(1) Joachim, C.; Gimzewski, J. K.; Aviram, A. Electronics Using Hybrid-Molecular and Mono-Molecular Devices. *Nature* **2000**, *408*, 541−548.

(2) Moresco, F.; Meyer, G.; Rieder, K. H.; Tang, H.; Gourdon, A.; Joachim, C. Conformational Changes of Single Molecules Induced by Scanning Tunneling Microscopy Manipulation: A Route to Molecular Switching. *Phys. Rev. Lett.* **2001**, *86*, 672−675.

(3) Kühnle, A.; Linderoth, T. R.; Hammer, B.; Besenbacher, F. Chiral Recognition in Dimerization of Adsorbed Cysteine Observed by Scanning Tunnelling Microscopy. *Nature* **2000**, *415*, 891−893.

(4) Rosei, F.; Schunack, M.; Naitoh, Y.; Jiang, P.; Gourdon, A.; Laegsgaard, E.; Stensgaard, I.; Joachim, C.; Besenbacher, F. Properties

of Large Organic Molecules on Metal Surfaces. *Prog. Surf. Sci.* **2003**, *71*, 95−196.
(5) Mukherji, D.; Müser, M. H. Possible Explanation of the Lambda-Shape Anomaly in Polymer Surface Diffusion. *Phys. Rev. E* **2006**, *74*, 010601−010604.
(6) Müser, M. H.; Urbakh, M.; Robbins, M. O. Statistical Mechanics of Static and Low-Velocity Kinetic Friction. *Adv. Chem. Phys.* **2003**, *126*, 187−272.
(7) Koch, N. Energy Levels at Interfaces Between Metals and Conjugated Organic Molecules. *J. Phys.: Condens. Matter* **2008**, *20*, 184008.184020.
(8) D'Amico, A.; Di Natale, C.; Macagnano, A.; Davide, F.; Mantini, A.; Tarizzo, E.; Paolesse, R.; Boschi, T. Technology and Tools for Mimicking Olfaction: Status of the Rome Tor Vergata Electronic Nose. *Biosens. Bioelectron.* **1998**, *13*, 395.
(9) Harima, Y.; Kodaka, T.; Okasaki, H.; Kanugi, Y.; Yamashita, Y.; Ishii, H.; Seki, K. A Relationship Between a Metal Work Function and a Diffusion Potential at Schottky Barriers in Photovoltaic Cells Based on a Molecular Semiconductor. *Chem. Phys. Lett.* **1995**, *240*, 345−350.
(10) Savenijc, T. J.; Moons, E.; Boschloo, G. K.; Goossens, A.; Schaafsma, T. J. Photogeneration and Transport of Charge Carriers in a Porphyrin p/n Heterojunction. *Phys. Rev. B* **1997**, *55*, 9685−9692.
(11) O'Neill, M. P.; Niemczyk, M. P.; Svec, W. A.; Gosztola, D.; Gaines, G. L., III; Wasielewski, M. R. Picosecond Optical Switching Based on Biphotonic Excitation of an Electron Donor-Acceptor-Donor Molecule. *Science* **1992**, *257*, 63−65.
(12) Olivier, M.; Berlier, K.; Jadot, R. Adsorption of Butane, 2-Methylpropane, and 1-Butene on Activated Carbon. *J. Chem. Eng. Data* **1994**, *39*, 770−773.
(13) Matsuura, I. The Adsorption of Butene, Butadiene, and Ammonia on UO_3 and Sb_2O_3 Catalysts. *J. Catal.* **1974**, *35*, 452−459.
(14) Yang, M.; Somorjai, G. A. Adsorption and Reactions of C6 Hydrocarbons at High Pressures on Pt(111) Single-Crystal Surfaces Studied by Sum Frequency Generation Vibrational Spectroscopy: Mechanisms of Isomerization and Dehydrocyclization of n-Hexane. *J. Am. Chem. Soc.* **2004**, *126*, 7698−7708.
(15) Wu, X.; Kobayashi, N.; Nanao, H.; Mori, S. Adsorption and Reaction of Cyclohexene and 1-Hexene on Nascent Gold Surface Formed by Friction. *Tribol. Lett.* **2005**, *18*, 239−244.
(16) Kondo, J. N.; Liquin, S.; Wakabayashi, K.; Domin, K. IR Study of Adsorption and Reaction of 1-Butene on H-ZSM-5. *Catal. Lett.* **1997**, *47*, 129−133.
(17) Granato, M. A.; Lamia, N.; Vlugt, T. J. H.; Rodríguez, A. E.; Mori, S. Adsorption Equilibrium of Isobutane and 1-Butene in Zeolite 13X by Molecular Simulation. *Ind. Eng. Chem. Res.* **2008**, *47*, 6166−6174.
(18) Yoda, E.; Kondo, J. N.; Domen, K. Detailed Process of Adsorption of Alkanes and Alkenes on Zeolites. *J. Phys. Chem. B* **2005**, *109*, 1464−1472.
(19) Maciver, D. S.; Zabor, R. C.; Emmett, P. H. The Adsorption of Normal Olefins on Silica-Alumina Catalysts. *J. Phys. Chem.* **1959**, *63*, 484−489.
(20) de Clerk, A. Effect of Oxygenates on the Oligomerization of FischerTropsch Olefins over Amorphous SilicaAlumina. *Energy Fuels* **2007**, *21*, 625−632.
(21) Barth, J. V.; Weckesser, J.; Cai, C.; Gunter, P.; Burgi, L.; Jeandupeux, O.; Kern, K. Building Supramolecular Nanostructures at Surfaces by Hydrogen Bonding. *Angew. Chem., Int. Ed.* **2000**, *39*, 1230−1234.
(22) Boal, A. K.; Ilhan, F.; DeRouchey, J. E.; Thurn-Albrecht, T.; Russel, T. P.; Rotello, V. M. Manipulation of Atoms Across a Surface at Room Temperature. *Nature* **2000**, *404*, 743−745.
(23) Marchenko, O.; Cousty, J. Molecule Length-Induced Reentrant Self-Organization of Alkanes in Monolayers Adsorbed on Au(111). *Phys. Rev. Lett.* **2000**, *84*, 5363−5366.
(24) Furukawa, M. Fabrication of Molecular Alignment at the Specific Sites on Cu(111) Surfaces Using Self-Assembly Phenomena. *Surf. Sci.* **2000**, *445*, L58−L63.
(25) Gimzewski, J. K.; Modesti, S.; Schlittler, R. R. Cooperative Self-Assembly of Au Atoms and C60 on Au(110) Surfaces. *Phys. Rev. Lett.* **1994**, *72*, 1036−1039.
(26) Murray, P. W.; Pedersen, M.; Laegsgaard, E.; Stensgaard, I.; Besenbacher, F. Growth of C60 on Cu(110) and Ni(110) Surfaces: C60-Induced Interfacial Roughening. *Phys. Rev. B* **1997**, *55*, 9360−9363.
(27) Nath, S. K.; Banaszak, B. J.; de Pablo, J. J. A New United Atom Force Field for α-Olefins. *J. Chem. Phys.* **2001**, *114*, 3612−3617.
(28) Kong, L.; Denniston, C.; Müser, M. H.; Qi, Y. Non-bonded Force Field for the Interaction Between Metals and Organic Molecules: A Case Study of Olefins on Aluminum. *Phys. Chem. Chem. Phys.* **2009**, *11*, 10195−10203.
(29) Nath, S. K.; Escobedo, F. A.; de Pablo, J. J. On the Simulation of VaporLiquid Equilibria for Alkanes. *J. Chem. Phys.* **1998**, *108*, 9905−9912.
(30) Martin, M. G.; Siepmann, J. I. Transferable Potentials for Phase Equilibria. 1. United-Atom Description of n-Alkanes. *J. Chem. Phys.* **1998**, *102*, 2569−2577.
(31) Errington, J. R.; Panagiotopoulos, A. Z. A New Intermolecular Potential Model for the n-Alkane Homologous Series. *J. Chem. Phys.* **1999**, *103*, 6314−6322.
(32) Nath, S. K.; de Pablo, J. J. Simulation of Vapor-Liquid Equilibria for Branched Alkanes. *Mol. Phys.* **2000**, *98*, 231−238.
(33) Jorgensen, W. L.; Madura, M. D.; Swenson, J. Optimized Intermolecular Potential Functions for Liquid Hydrocarbons. *J. Am. Chem. Soc.* **1984**, *106*, 6638−6646.
(34) Spyriouni, T.; Economou, I. G.; Theodorou, D. N. Molecular Simulation of α-Olefins Using a New United-Atom Potential Model: VaporLiquid Equilibria of Pure Compounds and Mixtures. *J. Am. Chem. Soc.* **1999**, *121*, 3407−3413.
(35) Kowalczyk, P.; Bhatia, S. K. Optimization of Slitlike Carbon Nanopores for Storage of hythane Fuel at Ambient Temperatures. *J. Phys. Chem. B* **2006**, *110*, 23770−23776.
(36) Dominguez, H. Self-Aggregation of the SDS Surfactant at a Solid-Liquid Interface. *J. Phys. Chem. B* **2007**, *111*, 4054−4059.
(37) Dominguez, H.; Gama Goicoechea, A.; Mendoza, N.; Alejandre, J. Computer Simulations of Surfactant Monolayers at Solid Walls. *J. Colloid Interface Sci.* **2006**, *297*, 370−373.
(38) Puri, P.; Yang, V. Effect of Particle Size on Melting of Aluminum at Nano Scales. *J. Phys. Chem. C* **2007**, *111*, 11776−11783.
(39) Forester, T. R.; Smith, W. *DL-POLY Package of Molecular Simulation*; CCLRC, Daresbury Laboratory: Daresbury, Warrington, England, 1996.
(40) Hoover, W. G. Canonical dynamics: Equilibrium Phase-Space Distributions. *Phys. Rev. A* **1985**, *31*, 1695−1704.
(41) Kong, L.; Denniston, C.; Müser, M. H. The Crucial Role of Chemical Detail fos Slip-Boundary Conditions: Molecular Dynamics Simulations of Linear Oligomers Between Sliding Aluminum Surfaces. *Modell. Simul. Mater. Sci. Eng.* **2010**, *18*, 034004−034021.
(42) de Beer, S.; Wennink, P.; van der Weide-Grevelink, M.; Mugele, F. Do Epitaxy and Temperature Affect Oscillatory Solvation Forces? *Langmuir* **2010**, *26*, 13245−13250.
(43) Dominguez, H. Structure of the SDS/1-Dodecanol Surfactant Mixture on a Graphite Surface: a Computer Simulation Study. *J. Colloid Interface Sci.* **2010**, *345*, 293−301.
(44) Askadskaya, L.; Rabe, J. P. Anisotropic Molecular Dynamics in the Vicinity of Order-Disorder Transitions in Organic Monolayers. *Phys. Rev. Lett.* **1992**, *69*, 1395−1398.
(45) Groszek, A. J. Do Epitaxy and Temperature Affect Oscillatory Solvation Forces? *Proc. R. Soc. London, A* **1970**, *314*, 473−498.
(46) Vadakkepatt, A.; Dong, Y.; Lichter, S.; Martini, A. Effect of Molecular Structure on Liquid Slip. *Phys. Rev. E* **2011**, *84*, 066311.
(47) Egberts, H. J. C. E.; Berendsen, J. Molecular Dynamics Simulation of a Smectic Liquid Crystal with Atomic Detail. *J. Chem. Phys.* **1988**, *89*, 3718−3733.